

Joule heating effect on Peristaltic transport of water-based copper oxide over an asymmetric channel in presence of slip effects

Asha. S. K¹ and Sunitha G²

^{1,2} Department of Mathematics, Karnatak University, Dharwad-580003, India
ashask@kud.ac.in ¹ and sunithag643@gmail.com ²

Abstract: This research paper is intended to study the nanoparticles shapes on peristalsis of Casson fluid in a channel flow by considering Joule heating effects. The study of such flows has various relevance applications in biomedical engineering and industries. Slip conditions is maintained at the velocity, temperature and nanoparticle concentration. The problem is modeled in terms of partial differential equations with suitable slip boundary conditions and then computed by using semi analytical technique known as Homotopy Analysis Method with Mathematica software. The influences of nanoparticles shape on velocity, pressure, temperature and nanoparticle concentration distributions are discussed with the help of graphs. Here, increase in Joule heating parameter enhance the fluid temperature and nanoparticle concentration decreases with an increasing Joule heating and also we observed that the different shapes has different thermal conductivity, but the lamina shaped nanoparticles have high thermal conductivity as compared to needle shaped nanoparticles.

Keywords: Peristaltic Transport, Joule heating, Copper oxide, Casson fluid, Shape factor, Slip conditions.

Nomenclature

\hat{X}, \hat{Y}	Cartesian coordinates
\hat{t}	Time
\hat{h}_1	Right wall
β_2	Thermal slip parameter
\hat{u}, \hat{v}	Velocity components
Re	Reynolds number
β	Casson fluid parameter
β_1	Velocity slip parameter
Sr	Soret number
\hat{p}	Pressure
\hat{h}_2	Left wall

\hat{T}	Temperature
Br	Nanoparticle Grashof number
$\hat{\phi}$	Nanoparticle concentration
β_3	Concentration slip parameter
Nt	thermophoresis diffusion parameter
T_m	Fluid mean temperature
K_{nf}	Effective thermal conductivity of the nanofluid
ρ_f	Base fluid density
Nb	Brownian motion parameter
Gr	Thermal Grashof number
ρ_s	Copper (II) oxide density
$(\rho C_p)_{nf}$	Heat capacitance
ρ_{nf}	Effective density
ϕ	Solid nanoparticle volume fraction
μ_{nf}	Effective dynamic viscosity
g	Acceleration due to gravity
α_{nf}	Effective thermal diffusivity
Q_0	Joule heating effect
$(\rho\beta)_{nf}$	the coefficient of thermal expansion
ψ	Stream function.

1. Introduction

The Analysis of peristaltic transport has great importance in biology and biomedicine. The biological applications are the vasomotion of small blood vessels such as venules, arterioles and capillaries, the process of swallowing of food through the esophagus and urine transport through the urethra. Latham [5] was first to investigate the peristaltic transport. Newtonian fluids in the wave frame and laboratory frame was studied by Shapiro et al [6] and Fung and Yih [7]. Some researchers [8-11] have investigated the peristalsis through different channel flows by considering Newtonian and non-Newtonian fluids.

The joule heating is referred to as electrically resistance heating or ohmic heating because of its relationship with ohm's law. Electric stoves, cartridge heaters, soldering irons, electric fuses and incandescent light (glows when the filament is heated by joule heating) are the important practical applications of Joule heating. Recent attempts on peristaltic transport with joule heating effect can be seen in references [12-15].

The nanofluids are a new type of fluids carried a very tiny number of nanoparticles are fixed effect in a carrier liquid. The thermal conductivity of the fluids is very low compared to solids. The term "nanofluid" was first introduced by Choi [16]. It indicates the engineered colloids composing the nanoparticles dispersed in a base fluid. The practical investigation has shown that the influence of nanoparticles has increasing the thermal conductivity depends on size as well as shape of the nanoparticles. The different shapes of the nanoparticles are Needle, Rods, Platelet, Spheres, Lamina and Bricks. Further analysis could be seen through references [17-20].

Motivated from the above discussion, the aim of the current research work is to analyze the influences of thermal radiation, magnetic field and porous medium on peristalsis of Casson fluid through channel flow under slip conditions. To the best of our knowledge, the discussion of the different nanoparticles shape effects of peristaltic flow with the Casson fluid, this has never been attempted before. Keeping pure water as the base fluid and Copper oxide as a selected nanoparticle in the peristaltic transportation has biological and industrial appliances. The basic governing equations have been simplified with infinite wavelength and low Reynolds number assumptions. The differential equations are simplified analytically by using Homotopy Analysis Method (HAM) [21-22]. The expressions for velocity, thermal energy and nanoparticle concentration have been computed. Analytical solutions that show the different physical parameters are shown in the graphical form.

2. Formulation of the problem

The geometry of model has considered the peristaltic transport of uniform thickness $d_1 + d_2$ on asymmetric channel. The sinusoidal travelling of the small amplitude waves a_1 and b_1 propagates the speed of the channel walls and s is the constant speed of the channel flow. The geometry of fluid model is defined as

$$\hat{Y} = \hat{h}_1 = a_1 \cos \left[\left(\hat{X} - s\hat{t} \right) \frac{2\pi}{\lambda} \right] + d_1, \quad (1)$$

$$\hat{Y} = \hat{h}_2 = -b_1 \cos \left[\left(\hat{X} - s\hat{t} \right) \frac{2\pi}{\lambda} + \omega \right] - d_2, \quad (2)$$

here a_1 and b_1 are the amplitudes of the channel flow, λ is wavelength of channel walls, \hat{t} is time, ω is the phase difference, we considering (\hat{X}, \hat{Y}) are the coordinate system, where \hat{X} and \hat{Y} are perpendicular to each other. Here d_2 and d_1 are satisfies the below condition.

$$a_1^2 + 2a_1b_1 \cos \omega + b_1^2 \leq (d_2^2 + d_1^2). \quad (3)$$

The Rheology of equations for an isotropic and incompressible flow of a Casson fluid can be expressed as follows

$$\tau_{ij} = \left(\mu_\beta + \frac{\rho_y}{\sqrt{2\Pi}} \right) 2e_{ij} \quad \text{when } \Pi > \Pi_c, \quad (4)$$

$$\tau_{ij} = \left(\mu_\beta + \frac{\rho_y}{\sqrt{2\Pi_c}} \right) 2e_{ij} \quad \text{when } \Pi < \Pi_c, \quad (5)$$

where τ_{ij} is the stress tensor of the fluid with $(i, j)^{\text{th}}$ components, $\Pi = e_{ij}e_{ij}$, e_{ij} is the deformation rate of $(i, j)^{\text{th}}$ component, ρ_y is the yield stress of the fluid, μ_β is dynamic plastic viscosity of the viscous fluid, Π_c is the critical value of the product based on viscous fluid.

Vector form of the velocity field v is given as,

$$V = \left(\hat{U}(\hat{x}, \hat{y}, \hat{t}), \hat{V}(\hat{x}, \hat{y}, \hat{t}) \right). \quad (6)$$

where $\hat{U}(\hat{x}, \hat{y}, \hat{t})$ and $\hat{V}(\hat{x}, \hat{y}, \hat{t})$ are the velocity components.

The dimensional governing equations for two-dimensional cartesian coordinate system can be expressed as

$$\frac{\partial \hat{U}}{\partial \hat{X}} + \frac{\partial \hat{V}}{\partial \hat{Y}} = 0, \quad (7)$$

$$\rho_{nf} \left(\frac{\partial \hat{U}}{\partial \hat{t}} + \hat{U} \frac{\partial \hat{U}}{\partial \hat{X}} + \hat{V} \frac{\partial \hat{U}}{\partial \hat{Y}} \right) = -\frac{\partial \hat{p}}{\partial \hat{X}} + \mu_{nf} \left(1 + \frac{1}{\beta} \right) \left(\frac{\partial^2 \hat{U}}{\partial \hat{X}^2} + \frac{\partial^2 \hat{U}}{\partial \hat{Y}^2} \right) + g(\rho\beta_T)_{nf} (\hat{T} - \hat{T}_0) + g(\rho\beta_C)_{nf} (\hat{C} - \hat{C}_0), \quad (8)$$

$$\rho_{nf} \left(\frac{\partial \hat{V}}{\partial \hat{t}} + \hat{U} \frac{\partial \hat{V}}{\partial \hat{X}} + \hat{V} \frac{\partial \hat{V}}{\partial \hat{Y}} \right) = -\frac{\partial \hat{p}}{\partial \hat{Y}} + \mu_{nf} \left(1 + \frac{1}{\beta} \right) \left(\frac{\partial^2 \hat{V}}{\partial \hat{X}^2} + \frac{\partial^2 \hat{V}}{\partial \hat{Y}^2} \right), \quad (9)$$

$$(\rho c_p)_{nf} \left(\frac{\partial \hat{T}}{\partial \hat{t}} + \hat{U} \frac{\partial \hat{T}}{\partial \hat{X}} + \hat{V} \frac{\partial \hat{T}}{\partial \hat{Y}} \right) = k_{nf} \left(\frac{\partial^2 \hat{T}}{\partial \hat{X}^2} + \frac{\partial^2 \hat{T}}{\partial \hat{Y}^2} \right) + D_{nf} k_T \left(\frac{\partial^2 \hat{C}}{\partial \hat{X}^2} + \frac{\partial^2 \hat{C}}{\partial \hat{Y}^2} \right) + Q_0, \quad (10)$$

$$\frac{\partial \hat{C}}{\partial \hat{t}} + \hat{U} \frac{\partial \hat{C}}{\partial \hat{X}} + \hat{V} \frac{\partial \hat{C}}{\partial \hat{Y}} = D_{nf} \left(\frac{\partial^2 \hat{C}}{\partial \hat{X}^2} + \frac{\partial^2 \hat{C}}{\partial \hat{Y}^2} \right) + \frac{D_{nf} k_T}{T_m} \left(\frac{\partial^2 \hat{T}}{\partial \hat{X}^2} + \frac{\partial^2 \hat{T}}{\partial \hat{Y}^2} \right), \quad (11)$$

where \hat{U} is the velocity component in \hat{X} coordinate and \hat{V} is the velocity component in \hat{Y} coordinate, σ_{nf} signifies the electrical conductivity, β_T and β_C are the coefficients of thermal expansion and solutal expansion, \hat{C} is the concentration of the nanoparticle, D_{nf} is the thermal diffusivity and T_m fluid mean temperature.

In equations (8)-(11), the heat capacitance $(\rho C_p)_{nf}$, effective dynamic viscosity μ_{nf} , effective density ρ_{nf} , effective thermal conductivity of the nanofluid is k_{nf} and the effective of thermal diffusivity α_{nf} are defined as

$$(\rho C_p)_{nf} = (1 - \phi)(\rho C_p)_f + \phi(\rho C_p)_s, \quad (12)$$

$$\mu_{nf} = \frac{\mu_f}{(1 - \phi)^{2.5}}, \quad (13)$$

$$\rho_{nf} = (1 - \phi)\rho_f + \phi\rho_s, \quad (14)$$

$$\alpha_{nf} = \frac{k_{nf}}{(\rho C_p)_{nf}}, \quad (15)$$

here β_f and β_s are the coefficients of thermal expansions of base fluid and nanoparticle, $(C_p)_s$ and $(C_p)_f$ are the heat capacities at a certain pressure and the Maxwell-Garnett [23] and further established Hamilton and Crosser model [24] to taken into account of random motion particle geometries by proposing a shape factor. On the basis of this model, when the larger thermal

conductivity of the nanoparticles is 100 times higher than the thermal conductivity of the base fluids, the thermal conductivity can be written as:

$$k_{nf} = k_f \left(\frac{k_s + (m+1)k_f - (m+1)(k_f - k_s)\phi}{k_s + (m+1)k_f + (k_f - k_s)\phi} \right), \quad (16)$$

where subscripts f and s denotes the base fluid phase and nanoparticles phase, k_f and k_s are the thermal conductivities of the base fluid and nanoparticle, respectively. m is the shape factor of the Hamilton-Crosser model [24] and the shape factor values of different shapes are noted in Table 1. The shape factor should be noted $m = \frac{3}{\lambda}$, here λ is the sphericity (the ratio between the surface areas of sphere and real particles with equal volumes). The sphericity of the needle and lamina are 0.62 and 0.185, respectively. The shape factor of the particle is 3 ($m=3$). In this case, Hamilton-Crosser model becomes a Maxwell- Garnett model. Thermophysical properties of Copper (II) oxide are mentioned in Table 2.

The wave and laboratory frames are introduced through

$$\hat{x} = \hat{X} - s\hat{t}, \quad \hat{u} = \hat{U} - s, \quad \hat{y} = \hat{Y}, \quad \hat{v} = \hat{V}. \quad (17)$$

The corresponding dimensional boundary conditions are

$$\left. \begin{aligned} \hat{\psi} = \frac{q}{2}, \hat{u} = \frac{\partial \hat{\psi}}{\partial \hat{Y}} = -s - \hat{\beta}_1 \left(1 + \frac{1}{\beta} \right) \frac{\partial^2 \hat{\psi}}{\partial \hat{Y}^2}, \hat{T} + \hat{\beta}_2 \frac{\partial \hat{T}}{\partial \hat{Y}} = \hat{T}_0, \hat{C} + \hat{\beta}_3 \frac{\partial \hat{C}}{\partial \hat{Y}} = \hat{C}_0 \text{ at } \hat{Y} = \hat{h}_1, \\ \hat{\psi} = -\frac{q}{2}, \hat{u} = \frac{\partial \hat{\psi}}{\partial \hat{Y}} = -s + \hat{\beta}_1 \left(1 + \frac{1}{\beta} \right) \frac{\partial^2 \hat{\psi}}{\partial \hat{Y}^2}, \hat{T} - \hat{\beta}_2 \frac{\partial \hat{T}}{\partial \hat{Y}} = \hat{T}_1, \hat{C} - \hat{\beta}_3 \frac{\partial \hat{C}}{\partial \hat{Y}} = \hat{C}_1 \text{ at } \hat{Y} = \hat{h}_2, \end{aligned} \right\} \quad (18)$$

The following non-dimensional parameters are

$$\left. \begin{aligned}
\psi &= \frac{\hat{\psi}}{sd_1}, X = \frac{\hat{X}}{\lambda}, Y = \frac{\hat{Y}}{d_1}, t = \frac{s\hat{t}}{\lambda}, x = \frac{\hat{x}}{\lambda}, \delta = \frac{d_1}{\lambda}, y = \frac{\hat{y}}{d_1}, u = \frac{\hat{u}}{s}, \theta = \frac{\hat{T} - \hat{T}_0}{\hat{T}_1 - \hat{T}_0}, \\
\gamma &= \frac{\hat{C} - \hat{C}_0}{\hat{C}_1 - \hat{C}_0}, h_1 = \frac{\hat{h}_1}{d_1}, h_2 = \frac{\hat{h}_2}{d_1}, d = \frac{d_2}{d_1}, a = \frac{a_1}{d_1}, b = \frac{b_1}{d_1}, v = -\delta \frac{\partial \psi}{\partial x}, u = \frac{\partial \psi}{\partial y}, \\
F &= \frac{q}{sd_1}, P = \frac{\hat{p}d_1^2}{s\lambda\mu_f}, \beta_1 = \frac{\hat{\beta}_1}{d_1}, \beta_2 = \frac{\hat{\beta}_2}{d_1}, \beta_3 = \frac{\hat{\beta}_3}{d_1}, Gr = \frac{g(\rho\beta T)_{nf}d_1^2(\hat{T}_1 - \hat{T}_0)}{s\mu_f}, \\
Br &= \frac{g(\rho\beta C)_{nf}d_1^2(\hat{C}_1 - \hat{C}_0)}{s\mu_f}, v = \frac{\hat{v}}{s}, Sr = \frac{D_{nf}k_T(\hat{C}_1 - \hat{C}_0)}{k_f(\hat{T}_1 - \hat{T}_0)}, Nb = \frac{(\rho c_p)_{nf}D_{Cf}(\hat{C}_1 - \hat{C}_0)}{(\rho c_f)_{nf}\mu_f}, \\
Nt &= \frac{(\rho c_p)_{nf}D_{Tf}(\hat{T}_1 - \hat{T}_0)}{(\rho c_f)_{nf}\mu_f T_m}, Re = \frac{\rho_f s d_1}{\mu_f}, Q_1 = \frac{Q_0 d_1^2}{(\hat{T}_1 - \hat{T}_0)k_f}.
\end{aligned} \right\} \quad (19)$$

By using the non-dimensional terms then the equations (8)-(11) can be written as

$$\frac{\partial p}{\partial x} = \frac{1}{(1-\phi)^{2.5}} \left(1 + \frac{1}{\beta}\right) \frac{\partial^2 u}{\partial y^2} + Gr\theta + Br\gamma, \quad (20)$$

$$\frac{\partial p}{\partial y} = 0, \quad (21)$$

$$\frac{1}{(1-\phi)^{2.5}} \left(1 + \frac{1}{\beta}\right) \frac{\partial^4 \psi}{\partial y^4} + Gr \frac{\partial \theta}{\partial y} + Br \frac{\partial \gamma}{\partial y} = 0, \quad (22)$$

$$A^* \frac{\partial^2 \theta}{\partial y^2} + Sr \frac{\partial^2 \gamma}{\partial y^2} + Q_1 = 0, \quad (23)$$

$$\frac{\partial^2 \gamma}{\partial y^2} + \frac{Nt}{Nb} \frac{\partial^2 \theta}{\partial y^2} = 0, \quad (24)$$

$$\text{where } A^* = \left[\frac{K_s + (m+1)K_f - (m+1)(K_f - K_s)\phi}{K_s + (m+1)K_f + (K_f - K_s)\phi} \right].$$

The corresponding dimensionless boundary conditions are

$$\left. \begin{aligned}
\psi &= \frac{F}{2}, u = \frac{\partial \psi}{\partial y} = -1 - \beta_1 \left(1 + \frac{1}{\beta}\right) \frac{\partial^2 \psi}{\partial y^2}, \theta + \beta_2 \frac{\partial \theta}{\partial y} = 0, \gamma + \beta_3 \frac{\partial \gamma}{\partial y} = 0 \text{ at } y = h_1 = a \cos[2\pi(x-t)] + 1, \\
\psi &= -\frac{F}{2}, u = \frac{\partial \psi}{\partial y} = -1 + \beta_1 \left(1 + \frac{1}{\beta}\right) \frac{\partial^2 \psi}{\partial y^2}, \theta - \beta_2 \frac{\partial \theta}{\partial y} = 1, \gamma - \beta_3 \frac{\partial \gamma}{\partial y} = 1 \text{ at } y = h_2 = -b \cos[2\pi(x-t) + \omega] - d.
\end{aligned} \right\} \quad (25)$$

Here we have considering F is the mean flow over a period is

$$\Theta = F + 1, \quad F = \int_{h_1}^{h_2} \frac{\partial \psi}{\partial y} dy, \quad (26)$$

where $\Theta = \frac{Q}{sd_1}$ and $F = \frac{q}{sd_1}$.

Table 1: Shape of the nanoparticles with their shape factors.

Nanoparticle type	Shape	Shape factor	Sphericity
Needle		4.9	0.62
Lamina		16.2	0.185

Table 2: Thermophysical properties of the nanofluid (CuO-water)

Properties	CuO	Base fluid (water)
Appearance	Black to Brown powder	White crystalline solid
Density (ρ)	6.31 g/cm ³	997.1
Heat Capacity (ρC_p)	531.80	4179.0
Thermal Conductivity k	76.50	0.6130
Prandtl Number (Pr)	-	6.20
Melting Point	1,201° C (2,194° F)	0.00°C (32.00° F, 273.15K)
Boiling Point	2,000° C (3,632° F)	99.98° C (211.96° F, 373.13K)

3. Method of Solution

Dimensionless equations (22)-(24) are solved by using Homotopy Analysis Method (HAM), then the initial approximations and equivalent auxiliary linear operator are obtained as

$$\psi_0(y) = \beta_1 \left(1 + \frac{1}{\beta} \right) \left[\frac{F}{2} \frac{y^3}{6} - \left(\frac{h_1 + h_2}{2} \right) \frac{y^2}{2} + \left(\left(\frac{h_1 + h_2}{4} \right) - \left(\frac{h_1^2 + h_2^2}{4} \right) \right) y \right] + \left(\frac{h_1^3 + h_2^3}{12} \right) + \left(\frac{(h_1 + h_2)(h_1^2 + h_2^2)}{8} \right) - \left(\frac{h_1 + h_2}{8} \right) \left((h_1 + h_2) - (h_1^2 + h_2^2) \right), \quad (27)$$

$$\theta_0(y) = \frac{2}{\beta_2} \left[\frac{h_1 + h_2}{2} - y \right], \quad (28)$$

$$\gamma_0(y) = \frac{2}{\beta_3} \left[\frac{h_1 + h_2}{2} - y \right]. \quad (29)$$

$$L_\psi = \frac{\partial^4}{\partial y^4}, \quad L_\theta = \frac{\partial^2}{\partial y^2}, \quad L_\gamma = \frac{\partial^2}{\partial y^2}. \quad (30)$$

Zeroth-order deformation equations are

$$(1-q)L_\psi [\psi(y,q) - \psi_0(y,q)] = qH_\psi h_\psi N_\psi [\psi(y,q), \theta(y,q), \gamma(y,q)], \quad (31)$$

$$(1-q)L_\theta [\theta(y,q) - \theta_0(y,q)] = qH_\theta h_\theta N_\theta [\theta(y,q), \gamma(y,q)], \quad (32)$$

$$(1-q)L_\gamma [\gamma(y,q) - \gamma_0(y,q)] = qH_\gamma h_\gamma N_\gamma [\gamma(y,q), \theta(y,q)], \quad (33)$$

in the above equations, h_ψ , h_θ and h_γ are the auxiliary parameters, the embedded parameter is $q \in [0,1]$, auxiliary linear operator L , H_ψ , H_θ and H_γ are the auxiliary functions. Nonlinear operators N_ψ , N_θ and N_γ can be written as

$$N_\psi [\psi(y,q), \theta(y,q), \gamma(y,q)] = \frac{1}{(1-\phi)^{2.5}} \left(1 + \frac{1}{\beta} \right) \frac{\partial^4 \psi(y,q)}{\partial y^4} + Gr \frac{\partial \theta(y,q)}{\partial y} + Br \frac{\partial \gamma(y,q)}{\partial y}, \quad (34)$$

$$N_\theta [\theta(y,q), \gamma(y,q)] = A^* \frac{\partial^2 \theta(y,q)}{\partial y^2} + Sr \frac{\partial^2 \gamma(y,q)}{\partial y^2} + Pr Q_1, \quad (35)$$

$$N_\gamma [\gamma(y,q), \theta(y,q)] = \frac{\partial^2 \gamma(y,q)}{\partial y^2} + \frac{Nt}{Nb} \frac{\partial^2 \theta(y,q)}{\partial y^2}. \quad (36)$$

The initial approximations $\psi_0(y,q)$, $\theta_0(y,q)$ and $\gamma_0(y,q)$ approaches to $\psi(y,q)$, $\theta(y,q)$ and $\gamma(y,q)$, respectively. The q values taken from 0 to 1. Mathematically,

$$\psi(y,0) = \psi_0(y), \quad \theta(y,0) = \theta_0(y), \quad \gamma(y,0) = \gamma_0(y) \quad (37)$$

$$\psi(y,1) = \psi(y), \quad \theta(y,1) = \theta(y), \quad \gamma(y,1) = \gamma(y)$$

n-order deformation equations of the given problem are

$$L_\psi [\psi_n(y) - \xi_n \psi_{n-1}(y)] = h_\psi R_n^\psi(y), \quad (38)$$

$$L_\theta [\theta_n(y) - \xi_n \theta_{n-1}(y)] = h_\theta R_n^\theta(y), \quad (39)$$

$$L_\gamma [\gamma_n(y) - \xi_n \gamma_{n-1}(y)] = h_\gamma R_n^\gamma(y). \quad (40)$$

with

$$R_n^\psi(y) = \frac{1}{(n-1)!} \frac{\partial^{n-1} N_\psi [\psi(y,q), \theta(y,q), \gamma(y,q)]}{\partial q^{n-1}} \Big|_{q=0}, \quad (41)$$

$$R_n^\theta(y) = \frac{1}{(n-1)!} \frac{\partial^{n-1} N_\theta [\theta(y,q), \gamma(y,q)]}{\partial q^{n-1}} \Big|_{q=0}, \quad (42)$$

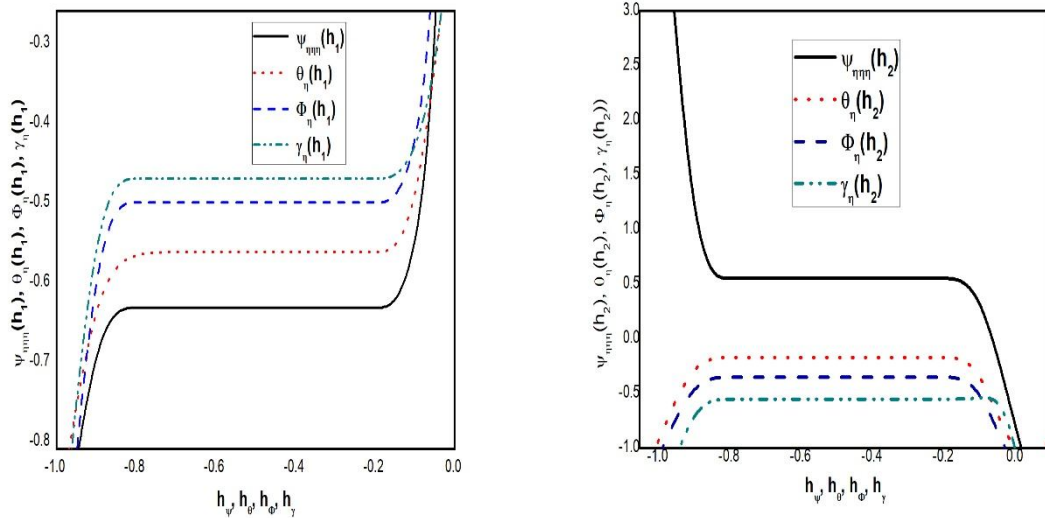
$$R_n^\gamma(y) = \frac{1}{(n-1)!} \frac{\partial^{n-1} N_\gamma [\gamma(y,q), \theta(y,q)]}{\partial q^{n-1}} \Big|_{q=0}, \quad (43)$$

where

$$\xi_n = \begin{cases} 0, & n \leq 1 \\ 1, & n > 1. \end{cases} \quad (44)$$

Convergence Analysis

In this section the convergence of Homotopy Analysis Method (HAM) are stated. $\psi(h_1)$, $\theta(h_1)$, $\Phi(h_1)$ and $\gamma(h_1)$ contains the auxiliary parameters h_ψ, h_θ and h_γ . Frame the \hbar -curves at 35th order approximation to find the proper values of h_ψ, h_θ and h_γ (see in figure 1(a & b)). The auxiliary linear parameters are adjusting and controlling the homotopic solutions. In this problem, we have chosen the convergence solution as $h_\psi = h_\theta = h_\gamma = -0.7$.



Figures 1(a) and 1(b): h curves for the function of $\psi(h_1)$, $\psi(h_2)$, $\theta(h_1)$, $\theta(h_2)$, $\gamma(h_1)$ and $\gamma(h_2)$ at 35th order approximations when $b = 0.5$, $t = 0.2$, $a = 0.5$, $x = 0.2$, $\beta_1 = 1.2$, $d = 1.5$, $\phi = 0.7$, $Br = 0.8$, $Gr = 0.8$, $Nt = 0.6$, $N_{TC} = 0.5$, $Q_1 = 1.5$, $\beta = 0.8$, $\beta_2 = 1.2$, $\beta_3 = 1.2$, $Nb = 0.6$.

4. Results and Discussion

This part of the research paper aims to discuss the velocity, thermal energy and concentration of the nanoparticles via graphs. The thermophysical properties of copper (II) oxide and water are mention in Table 2 and the different nanoparticle shapes and shape factor are noted in Table 1.

The impacts of physical parameters like Nanoparticle Grashof number Br , joule heating effect, velocity slip effect β_1 , Thermal Grashof number Gr , thermophoresis diffusion parameter Nt , Casson fluid parameter β , Soret number Sr , Brownian motion parameter Nb , thermal slip parameter β_2 , nanoparticle slip parameter β_3 on velocity, temperature and nanoparticle concentration of cupric oxide nanoparticles containing different shapes of nanoparticles, i.e., needle and lamina are analyzed. The influence of physical parameters is represented by the graphs in various colors. Further, the increase or decrease in physical quantities for various fluid flow parameters is shown by the direction of arrows.

4.1. Velocity Distribution

The influence of several flow parameters on velocity field are show in figs. 2 (a)-(d). These figures observed that velocity field traces a parabolic trajectory with the middle of channel is maximum. Figure 2(a) exhibits the velocity profile for various values of Casson fluid β . The Casson fluid parameter β increases with an enhancing the velocity profile. Physically, rising values of β develop the viscous forces. These viscous forces have propensity to reduce the thermal boundary layer. In the figure 2(b) shows that the velocity slip parameter β_1 on velocity. It is found the velocity slip parameter β_1 increase with an increasing the velocity field. Figure 2(c) depicts the impact of thermal Grashof number Gr on the velocity field. Form the figure 2(c), we have observed that the velocity enhanced with higher values of Gr . Physically, the buoyancy force of the fluid flow can be increases to the higher values thermal Grashof number because free convection influences. Figure 2(d) examines the influence of nanoparticle Grashof number Br on velocity. We have observed increasing the nanoparticle Grashof number then the velocity is enhanced.

4.2. Temperature profile

Figures 3(a)-(e) show variation of temperature profile as a function of y . Here variations of joule heating effect, thermophoresis parameter Nt , thermal slip parameter β_2 , solet number and Brownian motion paramter Nb are seen.

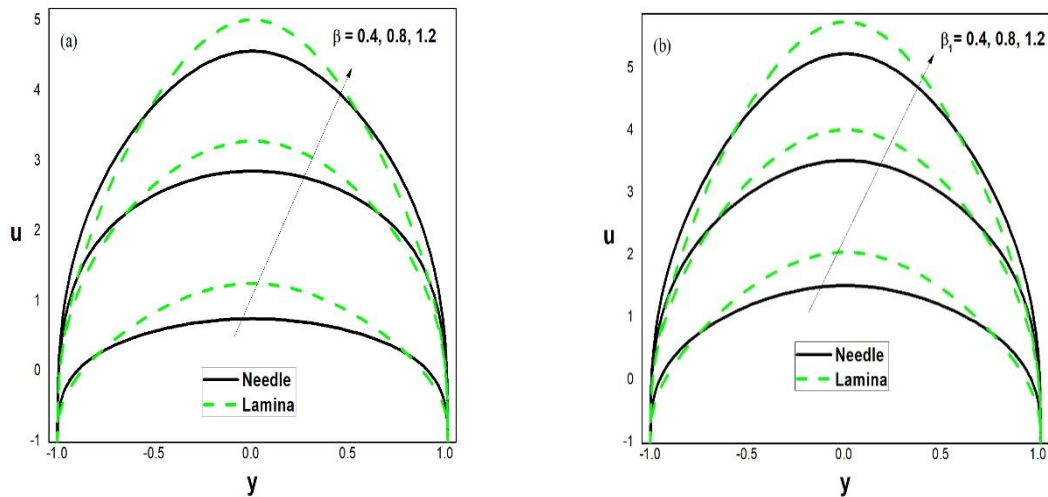
Figure 3(a) shows the impact of thermal slip parameter β_2 on the thermal energy. The thermal energy enhanced with an increasing thermal slip parameter β_2 . Figure 3(b) depicts the effect of solet number on thermal energy, here higher values of solet number with an increases the thermal energy. Figure 3(c) and figure 3(d) examines the temperature profile with various values of thermophoresis and Brownian motion paramters. These figures examines the therma enengy increases with an increasing Brownian motion parameter but opposite behaviour of the thermohoresis parameter and the physical reson is that the Brownian motion gives rise to the nanoparticles to rearrange, forming a blend, which enhancing the thermal conductivity. In the figure 3(e) examine the joule heating effect on temperature profile. It is found the joule heating effect increases with an increasing the temperature profile.

4.3. Nanoparticle concentration profile

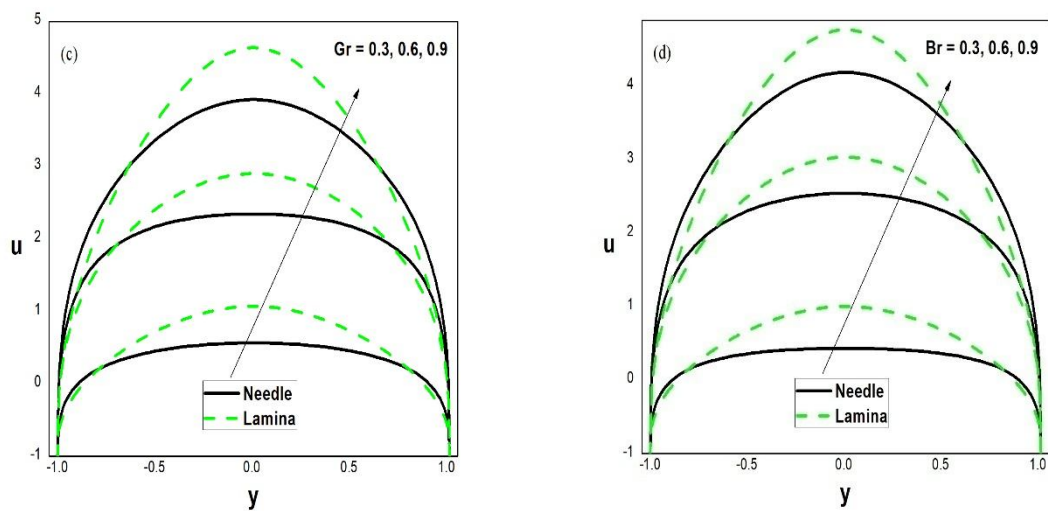
Figures 4 (a)-(d) show the behavior of nanoparticle concentration for the variation of joule heating effect, thermal slip parameter β_2 , solet number, thermophoresis parameter and Brownian motion paramter.

Figure 4 (a) analyze the influence of concentration slip parameter β_2 on nanoparticle concentration. The results show that decreasing in temperature profile presences in a specific domain with increasing the Slip parameter β_2 . After that domain, the relationship is reflected with the Slip parameter β_2 . The figures 4 (b) and 4 (c) are examines the influence of the Nb and Nt on the nanoparticle concentration. It is examining that by increasing Nb , the concentration of nanoparticle decreases. However, an opposite trend has been observed as Nt . This is because, the random motion of nanoparticles getting increased with an increasing Nb , which in turn an enhancement of fluid temperature and reduction of the nanoparticle diffusion.

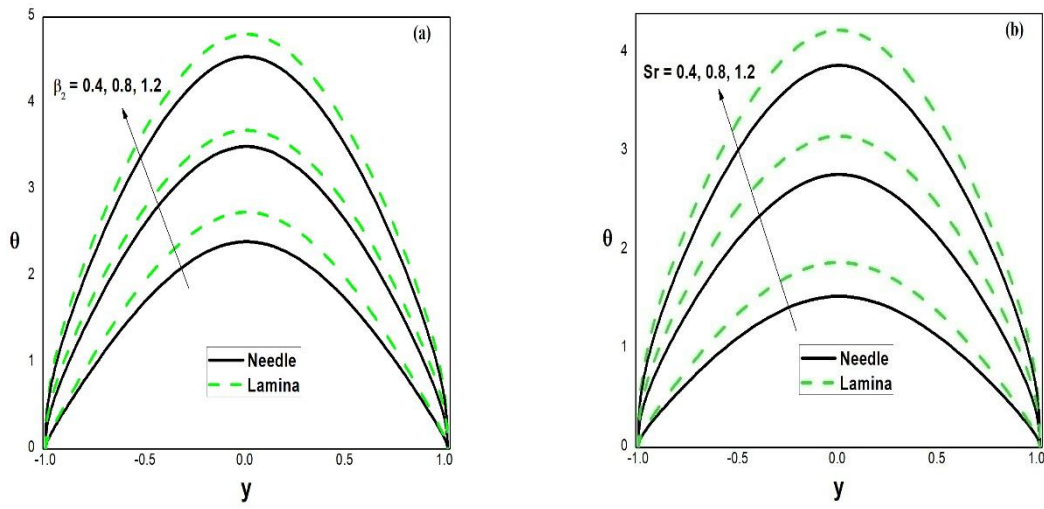
It is noticed from figure 4 (d) examine joule heating on nanoparticle concentration profile, here higher values of joule heating effect with an decreases the nanoparticle concentration.



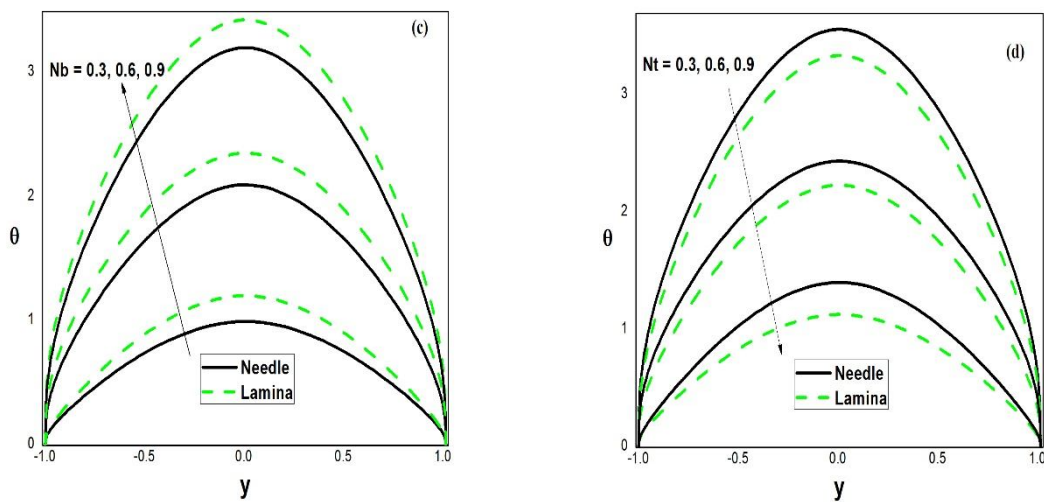
Figures2(a)-(b): variation of velocity profile versus y .when $b = 0.5$, $t = 0.2$, $x = 0.2$, $a = 0.5$, $d = 1.5$, $Sr = 0.8$, $Nt = 0.6$, $Q_1 = 1.5$, $Nb = 0.6$, $\beta_2 = 1.2$, $\beta_3 = 1.2$ and $\omega = 0.7$. (a) $Br = 0.8$, $Gr = 0.8$ and $\beta_1 = 1.2$. (b) $Br = 0.8$, $Gr = 0.8$ and $\beta = 0.7$.



Figures2(c)-(d): variation of velocity profile versus y .when $b = 0.5$, $t = 0.2$, $x = 0.2$, $a = 0.5$, $d = 1.5$, $Sr = 0.8$, $Nt = 0.6$, $Q_1 = 1.5$, $Nb = 0.6$, $\beta_2 = 1.2$, $\beta_3 = 1.2$ and $\omega = 0.7$. (c) $Br = 0.8$, $\beta = 0.7$ and $\beta_1 = 1.2$. (d) $Gr = 0.8$, $\beta = 0.7$, $\beta_1 = 1.2$.



Figures3(a)-(b): variation of temperature profile versus y . when $b = 0.5$, $t = 0.2$, $x = 0.2$, $a = 0.5$, $\beta_3 = 1.2$, $d = 1.5$ and $\omega = 0.7$. (a) $Nt = 0.6$, $Q_1 = 1.5$, $Nb = 0.6$ and $Sr = 0.8$. (b) $Nt = 0.6$, $Q_1 = 1.5$, $Nb = 0.6$ and $\beta_2 = 1.2$.



Figures3(c)-(d): variation of temperature profile versus y . when $b = 0.5$, $t = 0.2$, $x = 0.2$, $a = 0.5$, $\beta_3 = 1.2$, $d = 1.5$ and $\omega = 0.7$. (c) $Nt = 0.6$, $Q_1 = 1.5$, $\beta_2 = 1.2$ and $Sr = 0.8$. (d) $\beta_2 = 1.2$, $Q_1 = 1.5$, $Nb = 0.6$ and $Sr = 0.8$.

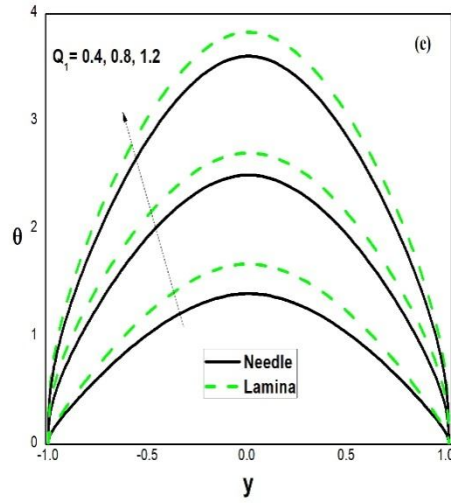
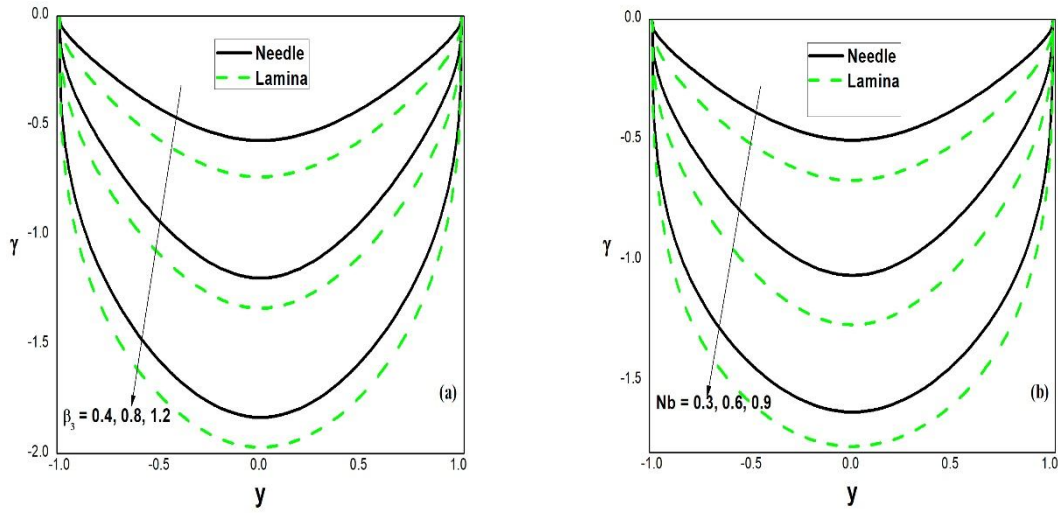
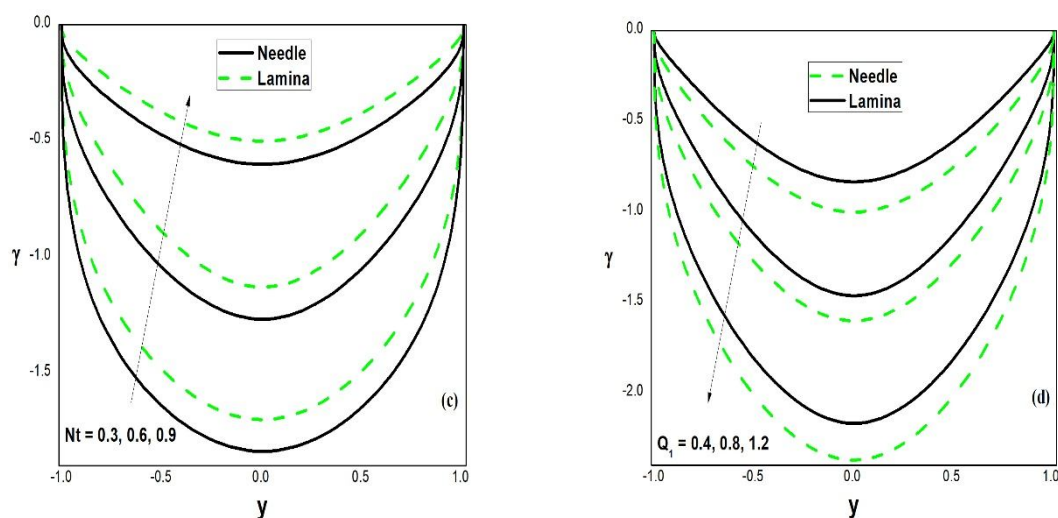


Figure 3(e): variation of temperature profile versus y . when $b = 0.5$, $t = 0.2$, $x = 0.2$, $a = 0.5$, $\beta_3 = 1.2$, $d = 1.5$ and $\omega = 0.7$. (e) $Nt = 0.6$, $\beta_2 = 1.2$, $Nb = 0.6$ and $Sr = 0.8$.



Figures 4(a)-(b) variation of nanoparticle concentration versus y . when $b = 0.5$, $t = 0.2$, $x = 0.2$, $Sr = 0.8$, $a = 0.5$, $\beta_2 = 1.2$, $d = 1.5$ and $\omega = 0.7$. (a) $Nt = 0.6$, $Nb = 0.6$ and $Q_1 = 1.5$. (b) $\beta_3 = 1.2$, $Nt = 0.6$ and $Q_1 = 1.5$.



Figures4(c)-(d): variation of nanoparticle concentration versus y .when $b = 0.5$, $t = 0.2$, $x = 0.2$, $Sr = 0.8$, $a = 0.5$, $\beta_2 = 1.2$, $d = 1.5$ and $\omega = 0.7$. (c) $\beta_3 = 1.2$, $Nb = 0.6$ and $Q_1 = 1.5$. (d) $Nt = 0.6$, $Nb = 0.6$ and $\beta_3 = 1.2$.

Conclusion

In the present research paper, joule heating effect on peristaltic transport of a slip condition with two different shapes of nanoparticles such as needle and lamina have been analyzed. The following important points observations were established:

- Increases in joule heating parameter enhances the fluid temperature and nanoparticle concentration decreases with an increasing joule heating effect.
- Increasing the velocity slip parameter generally accelerates the velocity of the fluid flow enhanced in different shapes at the middle of the channel and the ends of the channel walls is reduced and lamina shape of the Copper (II) oxide water is greater than needle shape. In the presence of fluid with nanoparticles, therefore assist the fluid flow.
- Both thermal and nanoparticle Grashof numbers enhance the velocity profile.
- The small change for the nanofluids containing nanoparticles shape needle is less observed as compared to containing nanoparticle shapelamina.The thermal conductivity of the nanoparticles is completely accordance with

expectation, the nanoparticles shape needle has very low thermal conductivity as compared to nanoparticle shape lamina.

References

- [1] Casson N (1959), A flow equation for pigment oil suspensions of the printing ink type. In *Rheology of Dispersed System*; Mill, C.C., Ed.; Pergamon Press: Oxford, UK.
- [2] Akbar N. S (2015), Influence of magnetic field on peristaltic flow of a Casson fluid in an asymmetric channel: application in crude oil refinement. *Journal of Magnetism and Magnetic Materials*. 378: 463–468.
- [3] ManjunathaGudekote and RajashekharChoudhari (2018), Slip Effects on Peristaltic Transport of Casson Fluid in an Inclined Elastic Tube with Porous Walls. *Journal of Advanced Research in Fluid Mechanics and Thermal Sciences*. 43 (1): 67-80.
- [4] Vajravelu K, Sreenadh S, Devaki P and Prasad K. V (2016), Peristaltic Pumping of a Casson Fluid in an Elastic Tube. *Journal of Applied Fluid Mechanics*. 9 (4): 1897-1905.
- [5] Latham T. W (1966), Fluid Motion in a Peristaltic Pump. M.S. Thesis, MIT, Cambridge.
- [6] Shapiro A. H, Jaffrin M. Y and Weinberg S.L (1969), Peristaltic Pumping with Long Wavelength at Low Reynolds Number. *Journal of Fluid Mechanics*. 17: 799-825.
- [7] Fung Y. C (1984), *Bio dynamics circulation*. (Springer-Verlag), New York Inc.
- [8] Asha S. K and Sunitha G (2017), Effect of couple stress in peristaltic transport of blood flow by homotopy analysis method. *AJST*. 12: 6958-6964.
- [9] Asha S. K and Sunitha G (2018), Mixed convection peristaltic flow of a Eyring-Powell nanofluid with magnetic field in a non-uniform channel. *JAMS*. 2(8): 332-334.
- [10] Asha S. K and Sunitha G (2019), Peristaltic Transport of Eyring-Powell nanofluid in a non-uniform channel. *Jordan Journal of Mathematics and Statistics*. 12(3): 431-453.
- [11] Asha S. K and Sunitha G (2019), Thermal radiation and Hall effects on peristaltic blood flow with double diffusion in the presence of nanoparticles. *Case studies in thermal engineering*. <https://doi.org/10.1016/j.csite.2019.100560>
- [12] Ravi kumar S, Suresh Goud J, Srilatha P, Sivaiah R and Abzal S. K (2018), Reaction Joule Heating and Thermal Radiation Effects on MHD Peristaltic Couple Stress Hemodynamic Fluid Model through an Inclined Channel with Chemical. *International Journal of Pure and Applied Mathematics*. 120 (5): 967-981.

- [13] Asghar S, Hussain Q, Hayat T and Alsaadi F (2014), Hall and ion slip effects on peristaltic flow and heat transfer analysis with Ohmic heating. *Applied Mathematics and Mechanics*. 35 (12): 1509-1524.
- [14] Hayat T, Farooq, Ahmad B and Alsaedi A (2016), Characteristics of convective heat transfer in the MHD peristalsis of Carreau fluid with Joule heating. *AIP Advances*. 6 (045302).
- [15] Asha S. K and Sunitha G (2019), Effect of Joule heating and MHD on peristaltic blood flow of Eyring–Powell nanofluid in a non-uniform channel. *Journal of Taibah University for Science*. 13(1): 155-168, DOI: 10.1080/16583655.2018.1549530.
- [16] Choi SUS (1995), Enhancing thermal conductivity of fluids with nanoparticles. *ASME fluids Eng Div*. 231: 99-105.
- [17] Liaqat Ali Khan, Mohsin Raza, Nazir Ahmad Mir and Rahmat Ellahi, Effects of different shapes of nanoparticles on peristaltic flow of MHD nanofluids filled in an asymmetric channel. *Journal of Thermal Analysis and Calorimetry*. <https://doi.org/10.1007/s10973-019-08348-9>
- [18] Noreen Sher Akbar and Adil Wahid Butt (2016), Ferromagnetic effects for peristaltic flow of Cu–water nanofluid for different shapes of nanosize particles. *Appl Nanosci*. 6:379–385 DOI 10.1007/s13204-015-0430-x
- [19] Palluru Devaki, Bhumarapu Venkateswarlu, Suripddi Srinivas and Sreedharamalle Sreenadh (2020), MHD Peristaltic flow of a nanofluid in a constricted artery for different shapes of nanosized particles. *Nonlinear Engineering*. 9: 51–59.
- [20] Noreen Sher Akbar, Adil Wahid Butt and Dharmendra Tripathi (2017), Nanoparticle shapes effects on unsteady physiological transport of nanofluids through a finite length non-uniform channel. *Results in Physics*. 7: 2477–2484.
- [21] Asha S. K and Sunitha G (2019), Influence of thermal radiation on peristaltic blood flow of a Jeffrey fluid with double diffusion in the presence of gold nanoparticles. *Informatics in medicine unlocked*. 17: 100272. <https://doi.org/10.1016/j.imu.2019.100272>
- [22] Asha Shivappa Kotnurkar and Sunitha Giddaiah (2019), Bioconvection peristaltic flow of a nano Eyring-Powell fluid containing gyrotactic microorganism. *SN Applied Sciences*. 1(1276): <https://doi.org/10.1007/s42452-019-1281-y>
- [23] Maxwell J. C (1904), *A Treatise on electricity and magnetism*, 3rd ed., Oxford Clarendon Press. U. K. 435.
- [24] Hamilton R. L and Crosser O. K (1962), *IEC Fundamentals*. 1:187.